

# RSC Advances



This is an *Accepted Manuscript*, which has been through the Royal Society of Chemistry peer review process and has been accepted for publication.

*Accepted Manuscripts* are published online shortly after acceptance, before technical editing, formatting and proof reading. Using this free service, authors can make their results available to the community, in citable form, before we publish the edited article. This *Accepted Manuscript* will be replaced by the edited, formatted and paginated article as soon as this is available.

You can find more information about *Accepted Manuscripts* in the [Information for Authors](#).

Please note that technical editing may introduce minor changes to the text and/or graphics, which may alter content. The journal's standard [Terms & Conditions](#) and the [Ethical guidelines](#) still apply. In no event shall the Royal Society of Chemistry be held responsible for any errors or omissions in this *Accepted Manuscript* or any consequences arising from the use of any information it contains.

## Mechanical Properties and Degradation Studies of Poly(Mannitol-Sebacate)/Cellulose Nanocrystal Nanocomposites

Águeda Sonseca<sup>1\*</sup>, Oscar Sahuquillo<sup>1</sup>, E. Johan Foster<sup>2</sup> and Enrique Giménez<sup>1</sup>

<sup>1</sup>Instituto de Tecnología de Materiales, Universitat Politècnica de València (UPV), Camino de Vera s/nº, 46022 Valencia (Spain)

<sup>2</sup>Virginia Tech, Department of Materials Science & Engineering, 445 Old Turner Street, 213 Holden Hall, Blacksburg VA 24061, USA

**\*To whom all correspondence should be addressed. Phone number; (+34)963879625; e-mail address; [agsonol@posgrado.upv.es](mailto:agsonol@posgrado.upv.es)**

### Abstract

Polyesters based on polyols and sebacic acid, known as poly(polyol sebacate) (PPS) are good candidates to develop degradable materials, due to their combination of flexibility and degradability, which are both useful properties in the context of soft-tissue engineering.<sup>1-4</sup> However, PPSs generally display poor mechanical properties, in particular low modulus, that limit the true potential of these materials in the biomedical field. Here, we introduce an approach to obtain nanocomposites based in poly(mannitol-sebacate) (PMS) matrices reinforced with cellulose nanocrystals (CNCs) in order to improve the application range of these materials. Different strategies were used based on varying the feed ratios between mannitol:sebacic acid (1:1 and 1:2), crosslinking conditions and CNC content, resulting in different degrees of crosslinking and, therefore, mechanical and degradation behavior. All of the developed nanocomposites displayed the expected mass loss during the degradation studies in simulated body fluid (SBF) similar to the neat matrix, however, doubling the sebacic acid feed ratio or extending the curing temperature and time, resulted in higher mechanical properties, structural

integrity, and shape stability during degradation time lessening mass loss rate. Changing mannitol:sebacic acid reaction rates from 1:1 to 1:2 and for low crosslinking degree neat samples, Young's modulus increases four-fold, while mass loss after 150 days of incubation is reduced by half. The Young's modulus range obtained with this process cover the range of human elastic soft tissues to tough tissues (0.7-200 MPa).

**Keywords:** Poly(polyol sebacate), cellulose nanocrystals, nanocomposites, mechanical properties, mass loss.

## Introduction

In the past few years, there has been steady progress in the development of biodegradable polymers for application in the medical field because these materials provide new opportunities to design less invasive and resorbable implants, tissue scaffolds, and medical devices that are able to avoid second revision surgeries, that limit the risk of infection and results in less trauma for the patient.<sup>5-8</sup> Moreover, biodegradable polymeric systems which offer the possibility to tailor their mechanical properties from soft to stiffer as well as the biodegradability ratio by varying the processing conditions also have additional advantages. Medical devices based on different classes of biodegradable polymers such as polyesters, polyanhydrides and polyurethanes have been widely investigated and some of them are commercially available as resorbable sutures, drug delivery systems, vascular grafts, wafers and orthopaedic fixation devices based, among others, on polylactic acid (PLA), polyglycolic acid (PGA), poly(lactic-co-glycolic acid) (PLGA), poly( $\epsilon$ -caprolactone) (PCL), poly(*p*-dioxanone) (PDO), or poly(trimethylene carbonate) (PTMC).<sup>9, 10</sup> However, most of these polymeric systems have degradation rates that are not optimal for short-medium term applications. For example, it takes more than 24 months for

poly( $\epsilon$ -caprolactones) and poly(L-lactic acid) to degrade in a biological environment, and from 2 to 24 months, depending on the ratio, for copolymers of polylactic acid (PLA) and polyglycolic acid (PGA). Also, the degradation rate for polyanhydrides is slow, around 12 months.<sup>6, 9, 11</sup> Moreover, these polymers have a lack of flexibility and elasticity at body temperature due to their high glass transition temperature and too high elastic modulus (400 MPa for PCL and 1200-3000 MPa for PLA)<sup>12</sup> that fail to mimic the elastic nature of many soft tissues such as blood vessels, cartilage, tendons or ligaments causing irritation, and sometimes damage, to the surrounding tissues.<sup>13-15</sup> To overcome these shortcomings, the development of novel biodegradable polyester elastomers, which are able to control their elastic properties and flexibility to better match with the elastic nature, biocompatibility and degradation profile of soft tissues, has increased considerably.<sup>16, 17</sup> Several researchers have synthesized polyester elastomers based on polyols such as 1,8-octanediol, ethylene glycol, butylene glycol, castor oil or glycerol, and carboxylic acids such as citric acid, ricinoleic acid, and sebacic acid,<sup>18-25</sup> which find application in soft tissue engineering as nerve-guidance, drug delivery, tissue adhesives and scaffolds to repair or replace body tissues.<sup>1-4, 19, 26, 27</sup> Poly(glycerol sebacate) (PGS) represents the most studied member of the poly-polyol sebacate (PPS) family, all of which are attractive because they are inexpensive and endogenous monomers found in human metabolism.<sup>27-29</sup> PGS is a randomly crosslinked polyester elastomer, whose design was motivated by the need to find biodegradable materials with tough mechanical properties.<sup>26</sup> Since PGS was firstly reported, several other polyols have been polymerized with sebacic acid to cover a wide range of mechanical properties and expand the spectrum of biomedical applications for these materials.<sup>16, 27, 30</sup> The most attractive synthetic feature of PPS is that through altering the stoichiometry of the diacid and polyol as well as varying the polycondensation conditions, the mechanical properties and degradation rates can be

easily tuned. Moreover, PPSs have biodegradability under physiological conditions and acceptable biocompatibility comparable to PLGA,<sup>16, 31</sup> and they have been reported as non-toxic based on *in vitro*<sup>32</sup> and *in vivo* studies.<sup>33</sup> These results indicate that these materials will be successful biomaterials with many biomedical applications. These thermoset elastomers have been reported to degrade via hydrolysis by surface erosion into metabolizable products, that maintain their structural integrity and geometric stability, and they are able to provide mechanical support during *in vivo* degradation.<sup>30, 33, 34</sup> The mechanical properties of PPS (tensile strength and elastic modulus) can be enhanced within a modest range by modifying the crosslink densities or in a much wider range by adjusting the stoichiometry. Nevertheless, to ensure an elongation at break higher than 10% (required for most tissue engineering applications), the range of Young's modulus for these materials (0.05-13 MPa) does not entirely cover that of living tissues such as skin (0.7-16 MPa), ligaments (1.5-54.5 MPa), tendons (1.5 GPa), or mandibular trabecular bone (6.9-200 MPa).<sup>14, 35, 36</sup> This fact limited their usefulness in applications where high strength and flexibility are required, such as ligating rubber bands for blood vessels or bones, elastomeric sutures, flexible coatings for stents, surgical devices, vascular grafts, surgical wound dressings, or catheters and small diameter tubes for drainage.<sup>37</sup> In this regard, we have reported in a previous work<sup>38</sup> that the addition of cellulose nanocrystals (CNC) as a reinforcing filler in a poly(mannitol-sebacate) (PMS) matrix with mannitol:sebacic acid ratio 1:1, is an effective approach to increase the strength and stiffness without compromising the elongation at break due to a strong affinity between matrix and filler, and the superior specific properties of the CNC (specific Young's modulus  $\sim 100$  GPa/cm<sup>3</sup>/g)<sup>39, 40</sup> compared with other nanofillers such as clays or bioceramics (Bioglass<sup>®</sup>). In that work, we developed 1:1 PMS nanocomposites with 1, 5 and 10 wt% of CNC using the solution casting

method followed by two different thermal crosslinking profiles, under low and high temperature-time conditions, to achieve samples with high and low degree of crosslinking. Mechanical, thermal, thermomechanical, and shape memory properties of the samples were then evaluated, and the results indicated that at least in a certain extent CNC interact with the matrix either, physically and chemically.<sup>41,42</sup> However, as was mentioned above, different ratio of mannitol and sebacic acid in PMS will hardly influence the properties of the matrix as well as the interactions with the filler. Therefore, to complete our previous study,<sup>38</sup> the aim of the present work is to develop PMS/CNC nanocomposites with mannitol:sebacic acid 1:2 stoichiometry, using the same CNC loading and crosslinking profiles than for previously reported 1:1 PMS stoichiometry, to compare how mechanical, thermal and degradation properties are affected. For PMS matrix with mannitol:sebacic acid 1:2 stoichiometry, we have also demonstrated that the residual alcohol groups of PMS matrix serve as ideal scaffolds for covalent tethering of chromophores with potential applications as bio-based up-converting rubbery systems for drug-delivery, bio-imaging, solar harvesting or displays.<sup>43</sup> This previous experience demonstrates the possibility to covalently attach chromophores to a PMS matrix. In this regard, PMS/CNC nanocomposites with 1:2 ratio were developed and final properties were tuned and evaluated taking into account the possibility to be influenced either by physical and chemical CNC/PMS interactions, but in a different way than for 1:1 PMS system, due to the stark differences of the matrices. Here we reported an approach build upon previous work, showing a study of PMS/CNC nanocomposites from mannitol:sebacic acid 1:1 and 1:2 reaction rates with low and high crosslinking degrees that were able to cover a wide range of mechanical properties and degradation rates for potential biomedical applications.

## Experimental section

**Materials.** Deuterated dimethylsulfoxide (DMSO-  $d_6$ ), dimethylformamide (DMF), sulfuric acid, sebacic acid (SA) (99% purity), and D-mannitol (MA) (99% purity), were purchased from Sigma Aldrich. Hydrochloric acid (HCl, 37% reagent grade) and sodium hydroxide (NaOH, 98% reagent grade) were purchased from Scharlau. Ultrapure water was directly taken from a Sartorius Stedim Arium 611 VF<sup>®</sup> water purification system ( $\rho = 18.2 \text{ m}\Omega\cdot\text{cm}$ ). Cellulose nanocrystals were isolated from cotton (Whatman No.1 filter paper) by controlled hydrolysis with sulphuric acid according to a protocol that is a modification of the method originally described by Dong et al.<sup>44</sup> This protocol introduces a small concentration of sulfate ester groups on the surface of the CNCs, which help to form stable suspensions in polar solvents.<sup>45</sup> Protocols followed to analyze dimensions, apparent crystallinity, crystal structure as well as the concentration of sulfate groups in the surface of the obtained CNC were previously reported,<sup>38</sup> and main results are collected in **Supporting Information Table S2**.

**Synthesis of poly(mannitol sebacate) (PMS) pre-polymer.** Sebacic acid (SA) and mannitol (MA) were reacted in a manner described previously.<sup>16</sup> Two poly(mannitol-sebacate) pre-polymers were first synthesized to obtain 1:1 and 1:2 mannitol:sebacic acid ratios. Poly(mannitol-sebacate) pre-polymer with a mannitol:sebacic acid 1:1 ratio was prepared following a previously described procedure.<sup>38</sup> To obtain the pre-polymer with a mannitol:sebacic acid 1:2 ratio,<sup>43</sup> appropriated molar amounts (0.034:0.069) of MA (6.21 g) and SA (13.79 g) were charged into a 250 mL three-necked round-bottom flask equipped with a stirrer and a condenser, which was placed in an oil heating bath and purged for 0.5 h with nitrogen. The temperature was slowly increased to 150 °C under continuous stirring and nitrogen flow to produce approximately 20 g of pre-polymer (**Scheme 1**). The reaction was stopped after 5 h (1 h

before gelation occurs), and the pre-polymer was dissolved in DMF (150 mg/mL), filtered and purified by dropwise precipitation into a four-fold excess of cold ultrapure water under continuous stirring. The precipitated pre-polymer was collected and dried under vacuum until no more solvent was detected in the infrared spectra. The yield of the reaction for 1:1 ratio was ~82%, while for 1:2 ratio was ~88%, as calculated from the weight of the monomers before reaction and the weight of each obtained pre-polymer after reaction.

**Characterization of PMS pre-polymers.** The  $^1\text{H-NMR}$  spectrum of 1:1 and 1:2 MA:SA ratio PMS pre-polymers were acquired in  $\text{DMSO-}d_6$  on a Varian Mercury VX-300 MHz NMR spectrometer (**Supporting Figure S1**). The compositions were determined from the ratio of the integrals of the signals associated with the mannitol and sebacic acid peaks<sup>16</sup> which reveal an incorporation of stoichiometric ratios mannitol:sebacic acid approximately of 1:1 and 1:2 (**Supporting Information Table S1**).

**Preparation of PMS/CNC nanocomposites.** The pre-polymers (1:1 and 1:2 MA:SA ratio) were first dissolved in DMF (100 mg/mL) by stirring at room temperature for 4 h. Suspensions of CNC at concentration of 10 mg/mL were prepared at appropriate ratio in DMF (designed to combine with 1.5 g of dry pre-polymers and form 1 wt%, 5 wt% and 10 wt% of PMS/CNC nanocomposites) by 40 min of ultrasonic treatment in a horn sonicator (Q500 sonicator, QSonica) with 1 sec on/off pulse conditions at a 20% amplitude. CNC suspensions were stirred with a PMS pre-polymer/DMF solution for 30 min and cast into aluminium Petri dishes (93 x 7 mm) and allowed to dry in an oven at 70 °C. Films consisting of the neat pre-polymers were prepared for reference purposes under the same conditions. The resulting pre-polymer/nanocomposites and the neat pre-polymer films were placed in a vacuum oven for further reaction. Two different curing profiles were applied to both pre-polymer/nanocomposites

series (1:1 and 1:2 MA:SA reaction rates), in which temperature and duration of the thermal treatment were varied to obtain samples with low and high degree of crosslinking and reaction rates 1:1 and 1:2. Samples with low degree of crosslinking were maintained at 120 °C for 72 hours under vacuum (60 cm Hg). Samples with high degree of crosslinking were obtained by using the same protocol and subsequently increasing the temperature to 170 °C while maintaining the vacuum (60 cm Hg) for a further 24 hours. Both procedures afforded films of ~ 150-200 µm of thickness.

**Transmission Electron Microscopy (TEM).** CNC TEM micrographs were recorded in a Phillips CM10 microscope with an accelerating voltage of 80kV. Samples were prepared by drying a drop of dilute whiskers suspension in H<sub>2</sub>O (0.1 mg/mL) onto a carbon-coated copper grid (Electron Microscopy Sciences) and subsequently dried under a heat lamp for 1 h.

**Differential Scanning Calorimetry (DSC).** Thermal behaviour of neat 1:1 and 1:2 PMS and their CNC nanocomposites was studied in a Mettler-Toledo DSC 800 under N<sub>2</sub> atmosphere. Samples were heated from -60 to 180 °C, cooled down to -60 °C and heated again to 180 °C at a heating/cooling rate of 10 °C/min under an N<sub>2</sub> atmosphere. The glass transition temperatures (T<sub>g</sub>) were calculated as the midpoint of the transition in the second heating run for all samples.

**Thermo gravimetric Analysis (TGA).** Thermal stability of all obtained samples and CNCs was recorded in a Mettler-Toledo TGA/SDTA 851 modulus analyser. The samples (5-10 mg) were weighted in zirconia crucibles and were heated in air at a rate of 10 °C/min from ambient temperature to 700 °C. Peak degradation temperatures were determined using the first derivative curve to determine the onset of thermal degradation.

**Swelling and degradation studies in SBF.** The swelling degree and degradation studies of all obtained samples ( $n=4$ , 5x5 mm, 150-200  $\mu\text{m}$  thickness) were studied under physiological conditions, in phosphate buffered saline solution (SBF) of  $7.4 \pm 0.5$  at 37 °C, prepared following a previously reported protocol.<sup>46</sup> For swelling studies, samples were collected after a 24 hour hydration period in SBF, blotted with a filter paper to remove excess surface water, and weighed (swelled weight;  $W_s$ ). The swelling percentage of the networks after 24 h was determined comparing the swelled weight ( $W_s$ ) with the initial weight ( $W_o$ ) using equation (1),

$$\text{Swelling degree}(\%) = \frac{W_s - W_o}{W_o} \times 100 \quad (1)$$

The degradation behaviour was determined by monitoring the weight loss at different times. Samples were weighed, immersed in 15 mL of SBF and incubated at 37 °C in an oven for various periods of time. Polymer samples were removed from SBF at different time intervals (14 days, 28 days, 42 days, 56 days and 150 days), thoroughly washed with ddH<sub>2</sub>O and dried under vacuum at 37 °C until constant weight was reached. The degradation degree of the polymers in SBF was calculated averaging the values of three samples by comparing the mass at each time interval ( $M_t$ ) with the initial mass ( $M_o$ ) using equation (2),

$$\text{Mass Loss} (\%) = \frac{M_o - M_t}{M_o} \quad (2)$$

**Fourier Transform Infrared Spectroscopy (FTIR).** FTIR transmission spectra were recorded for all neat 1:1 and 1:2 PMS and their CNC nanocomposites, using a Thermo Nicolet 5700 spectrometer, between 500-4500  $\text{cm}^{-1}$  with a 4  $\text{cm}^{-1}$  resolution and an Attenuated Total Reflectance (ATR) cell. Backgrounds were acquired before every 3<sup>rd</sup> sample. All samples were

vacuum-dried before measurement. FTIR spectra of neat 1:1 and 1:2 PMS with low and high crosslinking degree samples after 150 days of immersion in SBF were also recorded.

**Mechanical Micro-Testing.** Tensile tests were carried out on a DEBEN microtester equipped with a 150 N load cell and operated at a crosshead speed of 0.4 mm/min at room temperature. Specimen dimensions were typically 15 x 4 mm x 150~200  $\mu\text{m}$ . The elongation to break, Young's modulus and ultimate tensile strength were analysed for samples at initial stage (day 0 of degradation). Young's modulus of degraded samples was analysed at different degradation stages (immersion in SBF at 37 °C for 1, 28 and 150 days). Degraded samples were taken out from SBF and immediately tested. The Young's modulus (E) was determined from the initial slope of the stress-strain curves in the strain range of 0-10% for samples with low degree of crosslinking and 0-5% for samples with high degree of crosslinking. For each sample, a minimum of 5 rectangular samples were tested and the mechanical data were averaged.

## Results and discussion

### **CHARACTERIZATION OF INITIAL SAMPLES**

***Synthesis of PMS Pre-polymers and its Nanocomposites with CNC.*** The preparation of the PMS/CNC nanocomposites (1:1 and 1:2 MA:SA reaction rates) were achieved in a two-step process. Soluble poly(mannitol-sebacate) pre-polymers with stoichiometric ratios of mannitol:sebacic acid 1:1 and 1:2 were formed via the polycondensation reaction between the appropriated molar amounts of sebacic acid and D-mannitol (**Scheme 1**). In this first stage, the esterification is preferentially dominated by the reaction of the primary hydroxyl groups from D-mannitol (situated at both ends) with the carboxylic acid groups from sebacic acid.<sup>47, 48</sup> The reactions were stopped before gelation occurred, thus affording two polyesters with

approximately the initial molar amounts incorporated during synthesis as was revealed by  $^1\text{H}$  NMR spectra (**Supporting Info. S1**). Nanocomposites with 1 wt%, 5 wt%, and 10 wt% CNC were subsequently prepared by solution-casting mixtures of the PMS1:1 and PMS1:2 pre-polymers and the CNC were cured in a second step under vacuum using two different curing profiles designed to prepare materials with low and high degree of crosslinking of each stoichiometric ratio, referred to in this paper as LC and HC, respectively. **Figure 1** and **Supporting Information Table S2** show TEM micrographs and the key properties of isolated CNCs used to develop the nanocomposites.

**FTIR Study.** In order to confirm the ester formation and the presence of CNC, the ATR-FTIR spectra of the neat PMS matrix and the PMS/CNC nanocomposites of 1:1 and 1:2 stoichiometric ratios prepared under a low and high degree of crosslinking conditions were recorded. **Figure 2** shows the most relevance bands for the neat PMS and PMS/CNC nanocomposite stoichiometric ratio 1:1 and 1:2. The neat PMS samples show the characteristic absorption bands for hydrogen-bonded hydroxyl groups ( $3500\text{-}3200\text{ cm}^{-1}$ ) and for carbonyl- stretching vibrations of the ester groups ( $1800\text{-}1600\text{ cm}^{-1}$ ) in the polymer backbone, thus confirming the formation of polyesters. The bands around  $2924\text{ cm}^{-1}$  and  $2852\text{ cm}^{-1}$  are assigned to methylene ( $-\text{CH}_2-$ ) groups for the diacid residue and are observed in all spectra. A peak close to  $1150\text{ cm}^{-1}$  is assigned to the  $-\text{CO}$  stretch associated with the ester groups (**Supporting Info. S2**).<sup>49</sup> Samples prepared under a low degree of crosslinking conditions (LC) for both stoichiometric ratios showed a broad and intense  $-\text{OH}$  stretch peak at  $3350\text{ cm}^{-1}$ , an acid peak at  $1705\text{ cm}^{-1}$ , and an ester peak at  $1740\text{ cm}^{-1}$ , thus revealing a substantial fraction of unreacted hydroxyl and acid groups. The  $-\text{OH}$  band intensity was lower for the 1:2 stoichiometric ratio while the acid peak ( $1705\text{ cm}^{-1}$ ) was more evident in accordance with the higher sebacic acid content and lower mannitol presence compared with the

1:1 ratio. All samples prepared under a high degree of crosslinking conditions showed a reduction absorption spectra related to the hydroxyls groups at  $3350\text{ cm}^{-1}$  a more distinct 1:2 ratio, and a more pronounced  $-\text{CO}$  stretch associated with the ester groups, thus indicating a higher degree of esterification between acid and hydroxyl groups. The FTIR spectra of the nanocomposites revealed a similar pattern; it was able to discern peaks associated with the  $\text{CNC}-\text{OH}$  close to  $3338\text{ cm}^{-1}$  in the samples with 5 and 10 wt% CNC.

**Mechanical testing.** To relate the incorporation of CNC and the different PMS ratios and crosslinking conditions to the mechanical properties of the PMS matrix, micro-tensile tests were carried out. The average tensile Young's modulus, ultimate tensile strength, and elongation at break and toughness for all samples are summarized in **Table 1**. Comparing the neat PMS matrices, as was expected, the average ultimate tensile strength (UTS) and Young's modulus increased with the feed ratio of the sebacic acid monomer and to a greater extent for samples with a high crosslinking degree. The PMS 1:1 with a low degree of crosslinking had average UTS of  $1.2\pm 0.7\text{ MPa}$  and a Young's modulus of  $1.8\pm 0.3\text{ MPa}$ , while for the high crosslinking degree these values increase to  $7.0\pm 0.6\text{ MPa}$  and  $54.4\pm 3.3\text{ MPa}$ , respectively. While doubling the feed ratio of the sebacic acid monomer, the crosslink density increased<sup>30</sup> and for low degree of crosslinking samples a four-fold enhancement in UTS ( $4.5\pm 0.7\text{ MPa}$ ) and Young's modulus ( $7.2\pm 0.1\text{ MPa}$ ) values were obtained compared with 1:1 stoichiometry. Elongation at break of these samples (low crosslinking degree) is also hardly affected by changing stoichiometry to 1:2 ratio being reduced by half. In contrast, high degree of crosslinking 1:2 PMS samples are the stiffer and stronger showing a higher Young's modulus for a comparable elongation to their 1:1 PMS counterpart, however, the enhancement in the mechanical properties comparing neat matrices with this crosslinking profile for both stoichiometric rates, is not as marked as occurs

for low degree of crosslinking samples. Thus altering monomer-feed ratio of sebacic acid (increasing it) in PMS elastomers resulted in a wide range of mechanical properties, whilst for high degree of crosslinking samples similar elongation at break is maintained with a slightly increase in the mechanical properties.

Regarding nanocomposites, the improvement of the Young's modulus and tensile strength by increasing the CNC content (**Table 1**) was appreciated for both stoichiometric rates and crosslinking profiles. As was happened in previously reported 1:1 PMS nanocomposites system, by applying the high crosslinking degree profile to 1:2 PMS (**Figure 3**) nanocomposites results in much stiffer and stronger samples than their low crosslinking degree counterparts, reaching the highest Young's modulus close to 170 MPa for 5 and 10 wt% of CNC loads. Same CNC content, produce in all 1:2 PMS nanocomposites a five-fold and nearly two-fold increase in Young's modulus, for low and high degree of crosslinking nanocomposites respectively, compared with the analogous samples of 1:1 PMS nanocomposites. Thus, at equal cellulose load, the PMS 1:2 nanocomposites showed higher enhancement in mechanical properties than the PMS 1:1 nanocomposites due to a higher crosslink density from the matrix. Surprisingly, for this stoichiometric ratio (1:2), the addition of a small amount of CNC (only 1 wt%) results in a noticeable increase in the Young's modulus of 54% and 109% for low and high crosslinking degree samples, respectively, over the neat matrix. However, the addition of 1 wt% of CNC in the 1:1 ratio does not produce as high reinforcement as in the 1:2 PMS matrix, thus having similar Young's modulus to the neat polymer.

Another remarkable effect reported in the previous work,<sup>38</sup> and in what differs the behaviour of nanocomposites with different stoichiometry, was that increasing the CNC content in the PMS 1:1 samples provided higher stiffness without significantly compromising the elongation at break

of the composites for both crosslinking profiles. This was related to a molecular level reinforcement induced by reactions between the nanoparticles with high hydroxyl functionality and the matrix during the second polycondensation step, which also occur for previously reported clays and CNC-reinforced polyurethane nanocomposites.<sup>50-52</sup> In contrast increasing the CNC content in PMS 1:2 matrix for both crosslinking profiles, results in higher stiffness whereas the elongation at break decreases, but not significantly. Therefore, the increase in mechanical properties without compromising the elongation at break in the 1:1 system are due to the presence of CNC nanoparticles in the matrix and from polymer molecules interacting physically and chemically with CNC surfaces; however, for the 1:2 system, the higher improvement in the mechanical properties, even for lower CNC contents, and the slight decrease in elongation at break, seem to be influenced by the higher crosslink density, together with the presence of well-dispersed stiff nanoparticles and CNC/CNC interactions, more than from polymer/CNC interactions.

The different behaviors observed in terms of stiffness, strength, and elongation at break between the 1:2 and 1:1 neat matrices with the CNC presence can be associated to the differences in the OH:COOH ratio. One must consider that CNC is highly –OH functional and capable to interact with the residual hydroxyl or acid groups from PMS. As was already reported, as the value of average functionality ( $f_{av}$ ) increases, the degree of polymerization also increases.<sup>47, 53</sup> For the 1:1 PMS, and 1:2 PMS, the  $f_{av}$  calculated using Pinner's equation<sup>53, 54</sup> was 1.3 and 2.6, respectively. This implies that for the 1:2 pre-polymer, the free reactive sites available after the first polycondensation step are probably lower than in the 1:1 pre-polymer due to the higher density of crosslinking that results in fewer possibilities to form PMS/CNC interactions during the extent of the second polycondensation step. In the same way, the high offset in stoichiometry between

available carboxylic acid and hydroxyl groups, is also responsible of losing the positive effect in the mechanical properties and elongation at break (tend to decrease) for the PMS 1:1 and 10 wt% of CNC nanocomposite with a high degree of crosslinking, as produce a loss of the polymer-filler synergistic effect.<sup>38, 55</sup>

**Swelling Studies.** The crosslinking density of the neat PMS and PMS/CNC nanocomposites was determined by evaluating the swelling degree after the 24h immersion of the samples in SBF at 37 °C. **Table** shows the swelling degree for the neat and nanocomposites samples and the 1:1 and 1:2 reaction ratios. Samples with a higher sebacic acid ratio have a lower swelling degree that reveals an increase of the crosslink density of the networks for the same curing conditions in agreement with the mechanical property results.<sup>30</sup> For example, the neat PMS 1:1 obtained with low crosslinking curing conditions, swells to  $17.7\pm 1.0$  % and to  $8.7\pm 0.5$ % cured with high crosslinking conditions, whereas changing the reaction ratio to 1:2 reduces the swelling degree to  $14.4\pm 1.0$  % and to  $5.1\pm 0.8$  for the low and high crosslinking degree of the neat PMS, respectively. Moreover, it seems that there are two clearly differentiated effects with the addition of CNC to the 1:1 and 1:2 neat PMS networks. In the case of the 1:1 ratio, the addition of CNC does not seem to significantly modify the swelling behavior of the neat matrix for low crosslinking degree nanocomposites, while it tends to slightly decrease for 1 and 5 wt% of CNC for high crosslinking degree samples. High crosslinking degree samples with 10 wt% of CNC have the higher swelling degree; this fact is in concordance with the observed mechanical behavior and could be ascribed to the loss of polymer-filler interactions due to the high offset in the stoichiometry. For 1:2 stoichiometric, it is more evident that the addition of CNCs results in a lower swelling degree for both curing conditions. The addition of 10 wt% of CNCs reduces the swelling degree to  $10.4\pm 0.8$  and  $2.1\pm 0.5$  for low and high crosslinking degree samples

respectively. These results indicate that for the 1:1 ratio samples, the crosslinking degree of 1 and 5 wt% CNC content nanocomposites, is mainly governed by the PMS matrix and CNC interactions, probably due to the excess of hydroxyl groups in the polymer backbone and the new introduction by the fillers, while higher CNC contents (10 wt%) offer an excess of hydroxyl groups that would favour the CNC/CNC interactions, thus reducing the polymer/polymer interactions and, hence, the crosslinking degree. In the case of samples with a higher sebacic acid feed ratio, the excess acid groups, instead of hydroxyl groups in the polymer backbone, are expected to provide additional esterification sites that, together with the hydroxyl groups available in the CNCs, seem to be the responsible for the reduction in the swelling degree with the increase of the CNC content; that is, at least in a certain extent, CNC can act as a chemical crosslinker to enhance the crosslinking between CNC and PMS chains.<sup>56</sup>

**Thermal Characterization (DSC and TGA).** The effect of the CNC addition and crosslinking profiles over the thermal stability of the samples and glass transition ( $T_g$ ) were investigated using DSC and TGA. **Table 1** shows the glass transition and the onset of degradation values obtained for each sample. **Figure S3** shows the second heating run thermograms for all the 1:1 and 1:2 PMS and PMS/CNC samples. In the case of thermal stability, the neat PMS and nanocomposites with a high degree of crosslinking revealed an increase of thermal stability for these curing conditions compared with their low crosslinking counterparts. Yet no marked differences in the thermal stability behavior were evidenced by comparing both reaction rates (1:1 and 1:2). Some of the nanocomposites containing 5–10 wt% of CNC showed a slightly lower degradation onset temperature than the neat PMS or 1 wt% CNC samples, most likely due to the lower onset degradation temperature associated with the CNC glycosyl units degradation starting at 220 °C.<sup>57</sup> Regarding the DSC results, there are two factors in the nanocomposites that could influence  $T_g$  in

opposite directions. First, for the same curing profile, all the high crosslinking degree samples had a  $T_g$  higher than the low crosslinking degree samples; that is, longer curing times and temperature derivatives in a higher degree of crosslinking, probably due to that hydrogen bonding and/or chemical crosslink was gradually intensified during thermal curing, which hinders the mobility of polymeric chains increases the  $T_g$ . Moreover,  $T_g$  tends to decrease by slightly increasing the CNC content for the 1:1 low crosslinking degree samples, thus becoming more prominent for high crosslinking and 1:2 ratio samples due to the disruption of polymeric network.<sup>49, 58</sup> This second phenomenon could be explained as follows: in the first step of the condensation there occurs an esterification dominated by the reaction of the primary hydroxyl groups founded at both ends of mannitol with carboxylic acid groups from sebacic acid, thus leaving a large amount of secondary –OH groups in the pre-polymer backbone and also an excess of free carboxylic acid groups for 1:2 ratio. For both systems, CNCs were added into the PMS pre-polymers at this point and were subject to low and high crosslinking conditions, which considerably changed the OH/COOH ratio. These variations in the initial stoichiometry reaction of the 1:1 and 1:2 ratios not only seemed to be responsible for CNC not increasing the  $T_g$  as was expected, but also shifting it to lower temperatures for nanocomposites.<sup>57</sup> Similar behavior was observed for polyurethanes reinforced with CNC and poly(glycerol sebacate) bioglass nanocomposites due to strong associations between the filler and matrix.<sup>50, 58</sup> The new interactions between polymer chains and CNCs which seem to be favoured by higher sebacic acid feed ratios, higher crosslinking conditions, and raising the filler contents, all of which could reduce the polymer/polymer interactions and, therefore, be responsible for lowering the  $T_g$ .

## CHARACTERIZATION OF DEGRADED SAMPLES

### Degradation in SBF

The degradation of nanocomposites was investigated under physiological conditions (SBF, 37 °C) over the period of 150 days, showing the well-known scission of ester bonds occurring in the polyester network.<sup>34, 59</sup>

**Figure 4** shows the obtained degradation rates that seem to be loosely correlated to the swelling and mechanical properties. Taking these results into account,, roughly, the highest degradation rates correspond to samples with the lowest mechanical properties and highest swelling degrees; thus, to the 1:1 low crosslinking degree samples and nanocomposites. Continuing with the observed trend, the 1:1 reaction rate samples with a high crosslinking degree have slightly slower degradation behavior than the 1:2 low crosslinking degree samples, while the slowest degradation rate was obtained for the high crosslinking degree 1:2 samples. Comparing both reaction rates, an increase in sebacic acid content increases the time required for degradation due to an extent in the crosslink density that can effectively reduce the degradation rate for the same curing profile. Interestingly, the presence of CNCs does not seem to have a great influence on the degradation rate of the neat polymer matrices. As was observed in previously reported systems,<sup>60</sup> the differences in mass loss between the two studied systems (1:1 and 1:2) could also be related to the higher presence of mannitol, which is more noticeable in the 1:1 low crosslinking degree samples, that increases the hydrolytic degradation rate and enhances water penetration into the polymer matrix. An increase in the crosslink density achieved by changing the mannitol:sebacic acid ratio from 1:1 to 1:2 (corresponding to more equal numbers of alcohol and carboxylic groups) was also reported to be an important factor to significantly decrease the mass loss.<sup>61</sup> The

results indicate considerable impact of the network structure on the degradation rates, which can be tuned or slowed by changing the stoichiometric ratio or crosslinking conditions without being affected by CNC presence. To confirm the degradation of the samples, **Figure 5** shows FTIR spectra's main bands of films immersed in SBF after 150 days. All the samples developed a new peak centred around  $1560\text{ cm}^{-1}$ , which is not present in the spectra of dry samples. This peak is characteristic of the stretch of carboxylate groups, indicating that some salts of carboxylic acid have been formed due to the hydrolysed ester bonds.<sup>62,63</sup>

### **Mechanical Properties of PMS/CNC in SBF Medium**

In order to evaluate the effect of physiological conditions over the tensile properties of the developed materials, we allowed the samples to hydrate/degrade in SBF at  $37\text{ }^{\circ}\text{C}$  for 1, 28 and 150 days and then subjected them to a micro-tensile test. The changes in Young's modulus over the degradation time for all the samples are shown in **Figure 6**. After 150 days of immersion, the 1:1 low crosslinking degree samples still mostly retained their shape but had completely lost their mechanical compliance and their testing and manipulation became impractical. The mechanical behavior under hydrated conditions of biomaterials is an important factor in determining their possible biomedical and biological applications<sup>59</sup> since a drastic reduction in the mechanical properties of conventional polyesters between dry and wet conditions, may induce an inflammatory response that enhances fibrous capsule formation.<sup>49</sup> Regarding to the developed materials, it was observed that all the samples had a similar Young's modulus after one day hydration under physiological conditions that demonstrated low differences between dry and wet conditions. As expected, for the low and high crosslinking degree of neat PMS 1:1 and its CNC nanocomposites, a prolonged incubation time of up to 30 days produced a significant drop in the Young's modulus compared with the 1:2 ratio samples due to the higher presence of

the hydrophilic nature mannitol unit.<sup>59</sup> In contrast, Young's modulus for the low and high crosslinking degree of 1:2 PMS samples and CNC nanocomposites is less deteriorated over time in culture media. Similar behaviors have been reported for the poly(xylitol-sebacate) 1:1 and 1:2 ratios elastomers.<sup>34</sup> The dependence of Young's modulus on the immersion time in culture medium revealed marked differences between 1:1 and 1:2 rates without a clear dependence with CNC content, except for the high crosslinking degree of 1:2 PMS and nanocomposites. These samples are able to retain the initial stiffness by increasing the CNC content over the degradation time, probably due to less deterioration of the network and motivated by a higher crosslink density.

In general, mechanical properties are expected to decrease with time for these systems; however, after long periods of incubation (150 days), the 1:2 neat PMS and nanocomposites with a high degree of crosslinking had an increased Young's modulus, yet the other samples tended to decrease or remain unchanged after 30 days of incubation. Similar phenomena was observed in poly(propylene fumarate) composites and were initially ascribed to the complexation of the carboxylic groups formed during degradation.<sup>64, 65</sup> In our case, it could probably be related to the generation of new crosslinking/interaction points in the network due to the scission of ester linkages that increase free carboxylic acid salts (**Figure 5**). The fact that it is only occurring for these samples poses the question of whether these new crosslinking/interaction points can be favoured for the higher network density, and within that, whether all the new available functional groups are closer and can easily interact.

There are a couple of important features that can be concluded from this degradation study: On the one hand, the synthesized materials cover a wide range of mechanical properties and, hence, may be used for biomedical and tissue engineering. For example, tough living tissues such as

tendon ( $E=143-2310$  MPa), human ligament ( $E=65-541$  MPa), or cancellous bone ( $E=20-500$  MPa)<sup>66</sup> have a Young's modulus comparable to the high crosslinking degree samples. In applications where the involved tissue is softer and more elastic, the low crosslinking degree samples could be offered similar mechanical compliance for some human elastic soft tissues such as knee articular cartilage ( $2.1-11.8$  MPa),<sup>67, 68</sup> cerebral vein ( $6.85$  MPa) and artery ( $15.6$  MPa), aortic valve leaflet ( $15\pm 6$  MPa)<sup>59</sup> or pericardium ( $20.4\pm 1.9$  MPa).<sup>69</sup> On the other hand, in the context of biomaterials applications, the design of mechanically stable materials over an extended period is of importance for tissue remodelling at the wound site.<sup>70, 71</sup> Regarding this highly desirable mechanical stability following implantation, the 1:2 reaction rate nanocomposites have the highest mechanical stability over a one month period, and could be good candidates for mechanical support to damaged tissues during the lag phase of the healing process. Finally, it should be pointed out that for long-term biomedical applications, one major requirement of any material is that must be biocompatible. Thus, it has to be able to stay in contact with living tissues without causing any cytotoxic or other derived side effects. Previous studies have investigated approaches to create PPS composites based on the introduction of inorganic components such as halloysite nanotubes (clays) or multi-walled carbon nanotubes (MWCNTs) with improved mechanical properties.<sup>70, 72, 73</sup> However, the main drawback derived from the use of these inorganic nanoparticles *in vivo* is their potential toxicity as well as the uncertain (or non-existent) mechanism of removal from the body.<sup>74</sup> By using organic based fillers these drawbacks could be lessen. In this regards, although CNC is known as non-biodegradable material for a long time, they have recently gained attention because exhibit low cytotoxicity with a range of animal and human cell types and no cytotoxicity at concentration ranges of  $\sim 50$   $\mu\text{g/mL}$  of CNC.<sup>74-79</sup> Mahmoud et al.<sup>80</sup> reported that any noticeable cytotoxic effect

on two different cell lines occurred during *in vitro* cellular studies of two differently charged CNCs (positively and negatively) suggesting possible applications in both drug delivery and bioimaging. Jia et al.<sup>81</sup> reported potential application of microcrystal cellulose (MCC) and CNC as a filler of electrospun cellulose acetate vascular tissue scaffolds to improve biocompatibility. Thus, although the present work should be biocompatible, given that both components have been previously tested separately, future investigations are needed to characterize the toxicology of these cellulose nanocomposites materials thorough *in vitro* and *in vivo* testing, to confirm the potential biomedical application. The *in vitro* studies reported until now highlight that CNCs hold great promise in a wide variety of biotechnological and biomedical applications especially in tissue engineering.<sup>82</sup>

## Conclusions

Several strategies have been employed to prepare biodegradable poly(mannitol-sebacate) based materials having a broad range of mechanical properties and degradation characteristics. These strategies are based on varying feed reaction ratios, crosslinking conditions or the addition of CNCs as reinforcing fillers to alter the degradation rates as well as to tailor the mechanical stiffness of the poly(mannitol-sebacate) from  $1.8 \pm 0.3$  MPa to  $167.5 \pm 5.0$  MPa. Compared to similar reported systems based in poly(glycerol-sebacate), addition of high contents of nano-clays or Bioglass<sup>®</sup> (10-20 wt%) are necessary to achieve Young's modulus close to 2 MPa. In this regard, the addition of CNC in poly(mannitol-sebacate) matrices combined with different stoichiometry and crosslinking profiles, results in a more efficient and remarkable improvement in mechanical properties well above of the enhancement obtained for other fillers. Reported systems containing Bioglass<sup>®</sup> tends to experiment a sudden drop in mechanical properties after one day of immersion in SBF medium almost getting back to the strength level of neat materials.

In comparison PMS/CNC nanocomposites, provides more reliable mechanical support materials without immediately loss of mechanical stability. The amorphous nature of materials prepared provides the retention of mechanical properties and shape stability during long periods of incubation which are beneficial as could allow the load to be transferred to the surrounding tissues considering the development of a possible biomedical device. Moreover, acceleration (or deceleration) of the mass loss in similar nanocomposites, have been typically achieved through varying the filler content, or crosslinking degree of the neat matrix, but to our knowledge, no studies about the affection of both variables together for the same nano-filler composition over the degradation behaviour have been reported. Mass lose rate was primary determined by the degree of the crosslink density of materials that demonstrate slower degradation with the increasing feed ratio of sebacic acid or thermal curing time and temperature. However, the presence of CNC does not slow or accelerate the mass loss of the matrix, that makes easy to predict the behavior of the material over the degradation period. In summary, the large number of variables to be applied during the synthesis of these nanocomposites provides a wide range of possible mechanical properties, which could be broadly employed in many biomedical applications that approximate those of soft and tough tissues. Moreover, in vivo experiments will also provide the indications of biocompatibility, and finally determine the real utility of these materials.

### **Associated content**

Supporting Information; CNC properties, <sup>1</sup>H-NMR, IR and DSC complementary studies.

### **Acknowledgements**

The authors gratefully acknowledge financial support received from Spanish Ministry of Economy and Competitiveness (Project MAT2010/21494-C03), as well as the support of FPU grant from MED (MED-FPU; AP2009-2482) and the Adolphe Merkle Foundation.

## References

- 1 Z. Sun, C. Chen, M. Sun, C. Ai, X. Lu, Y. Zheng, B. Yang and D. Dong, *Biomaterials*, 2009, **30**, 5209-5214.
- 2 C. Sundback, J. Shyu, Y. Wang, W. Faquin, R. Langer, J. Vacanti and T. Hadlock, *Biomaterials*, 2005, **26**, 5454-5464.
- 3 D. Motlagh, J. Yang, K. Lui, A. Webb and G. Ameer, *Biomaterials*, 2006, **27**, 4315-4324.
- 4 A. Mahdavi, L. Ferreira, C. Sundback, J. W. Nichol, E. P. Chan, D. J. D. Carter, C. J. Bettinger, S. Patanavanich, L. Chignozha, E. Ben-Joseph, A. Galakatos, H. Pryor, I. Pomerantseva, P. T. Masiakos, W. Faquin, A. Zumbuehl, S. Hong, J. Borenstein, J. Vacanti, R. Langer and J. M. Karp, *Proc. Natl. Acad. Sci. U. S. A.*, 2008, **105**, 2307-2312.
- 5 I. Vroman and L. Tighzert, *Materials*, 2009, **2**, 307-344.
- 6 B. D. Ulery, L. S. Nair and C. T. Laurencin, *J. Polym. Sci., Part B: Polym. Phys*, 2011, **49**, 832-864.
- 7 L. Xue and H. P. Greisler, *J. Vasc. Surg.*, 2003, **37**, 472-480.
- 8 L. S. Nair and C. T. Laurencin, *Prog. Polym. Sci.*, 2007, **32**, 762-798.
- 9 P. A. Gunatillake and R. Adhikari, *Eur. Cell. Mater.*, 2003, **5**, 1-16.
- 10 J. C. Middleton and A. J. Tipton, *Biomaterials*, 2000, **21**, 2335-2346.
- 11 K. Athanasiou, C. Agrawal, F. Barber and S. Burkhart, *Arthroscopy*, 1998, **14**, 726-737.
- 12 I. Engelberg and J. Kohn, *Biomaterials*, 1991, **12**, 292-304.
- 13 Q. Chen, A. Bismarck, U. Hansen, S. Junaid, M. Q. Tran, S. E. Harding, N. N. Ali and A. R. Boccaccini, *Biomaterials*, 2008, **29**, 47-57.
- 14 S. Liang, W. D. Cook, G. A. Thouas and Q. Chen, *Biomaterials*, 2010, **31**, 8516-8529.
- 15 M. A. Meyers, P. Chen, A. Y. Lin and Y. Seki, *Prog. Mater. Sci.*, 2008, **53**, 1-206.

- 16 J. P. Bruggeman, B. de Bruin, C. J. Bettinger and R. Langer, *Biomaterials*, 2008, **29**, 4726-4735.
- 17 Y. Li, G. A. Thouas and Q. Chen, *RSC Adv.*, 2012, **22**, 8229-8242.
- 18 J. Yang, A. Webb, S. Pickerill, G. Hageman and G. Ameer, *Biomaterials*, 2006, **27**, 1889-1898.
- 19 J. Yang, A. Webb and G. Ameer, *Adv Mater*, 2004, **16**, 511-516.
- 20 H. Park, J. Seo, H. Lee, H. Kim, I. B. Wall, M. Gong and J. C. Knowles, *Acta Biomater.*, 2012, **8**, 2911-2918.
- 21 Z. Sun, L. Wu, X. Lu, Z. Meng, Y. Zheng and D. Dong, *Appl. Surf. Sci.*, 2008, **255**, 350-352.
- 22 Q. Liu, T. Tan, J. Weng and L. Zhang, *Biomed. Mater.*, 2009, **4**, 025015.
- 23 M. Y. Krasko, A. Shikanov, A. Ezra and A. J. Domb, *J. Polym. Sci., Part A: Polym. Chem.*, 2003, **41**, 1059-1069.
- 24 P. S. Sathiskumar and G. Madras, *Polym. Degrad. Stab.*, 2011, **96**, 1695-1704.
- 25 I. Djordjevic, N. R. Choudhury, N. K. Dutta and S. Kumar, *Polymer*, 2009, **50**, 1682-1691.
- 26 Y. Wang, G. Ameer, B. Sheppard and R. Langer, *Nat. Biotechnol.*, 2002, **20**, 602-606.
- 27 D. G. Barrett and M. N. Yousaf, *Molecules*, 2009, **14**, 4022-4050.
- 28 K. Ellwood, *Am. J. Clin. Nutr.*, 1995, **62**, 1169-1174.
- 29 S. Natah, K. Hussien, J. Tuominen and V. Koivisto, *Am. J. Clin. Nutr.*, 1997, **65**, 947-950.
- 30 J. P. Bruggeman, C. J. Bettinger, C. L. E. Nijst, D. S. Kohane and R. Langer, *Adv. Mater.*, 2008, **20**, 1922-1927.
- 31 S. Liang, W. D. Cook, G. A. Thouas and Q. Chen, *Biomaterials*, 2010, **31**, 8516-8529.
- 32 C. Bettinger, E. Weinberg, K. Kulig, J. Vacanti, Y. Wang, J. Borenstein and R. Langer, *Adv. Mater.*, 2006, **18**, 165-169.
- 33 Y. Wang, Y. Kim and R. Langer, *J. Biomed. Mater. Res. Part A*, 2003, **66A**, 192-197.
- 34 J. P. Bruggeman, C. J. Bettinger and R. Langer, *J. Biomed. Mater. Res. A*, 2010, **95A**, 92-104.
- 35 K. Firoozbakhsh, I. Yi, M. Moneim and Y. Umada, *Clin. Orthop.*, 2002, , 240-247.

- 36 S. K. Ha, *Med. Eng. Phys.*, 2006, **28**, 534-541.
- 37 V. R. Sastri, *Plastics in Medical Devices*, William Andrew Publishing, Boston, 2nd edn., 2010, pp. 217-262.
- 38 A. Sonseca, S. Camarero-Espinosa, L. Peponi, C. Weder, E. J. Foster, J. M. Kenny and E. Gimenez, *J. Polym. Sci. Part A: Polym. Chem.*, 2014, **52**, 3123-3133.
- 39 R. Rusli and S. J. Eichhorn, *Appl. Phys. Lett.*, 2008, **93**, 033111.
- 40 C. C. Sun, *J. Pharm. Sci.*, 2005, **94**, 2132-2134.
- 41 J. S. Haghpanah, R. Tu, S. Da Silva, D. Yan, S. Mueller, C. Weder, E. J. Foster, I. Sacui, J. W. Gilman and J. K. Montclare, *Biomacromolecules*, 2013, **14**, 4360-4367.
- 42 M. Jorfi, M. N. Roberts, E. J. Foster and C. Weder, *ACS Appl. Mater. Interfaces*, 2013, **5**, 1517-1526.
- 43 S. Lee, A. Sonseca, R. Vadrucci, E. Gimenez, E. J. Foster and Y. Simon, *J. Inorg. Organomet. Polym. Mater.*, 2014, **24**, 898-903.
- 44 X. Dong, T. Kimura, J. Revol and D. Gray, *Langmuir*, 1996, **12**, 2076-2082.
- 45 B. Braun and J. R. Dorgan, *Biomacromolecules*, 2009, **10**, 334-341.
- 46 T. Kokubo, H. Kushitani, S. Sakka, T. Kitsugi and T. Yamamuro, *J. Biomed. Mater. Res.*, 1990, **24**, 721-734.
- 47 R. Maliger, P. J. Halley and J. J. Cooper-White, *J Appl Polym Sci*, 2013, **127**, 3980-3986.
- 48 Q. Chen, *Biomedical Materials and Diagnostic Devices*, ed. A. Tiwari, M. Ramalingam, H. Kobayashi and A. P. F. Turner, John Wiley & Sons, Inc., MA, USA, 2012, pp. 529-560.
- 49 A. Patel, A. K. Gaharwar, G. Iviglia, H. Zhang, S. Mukundan, S. M. Mihaila, D. Demarchi and A. Khademhosseini, *Biomaterials*, 2013, **34**, 3970-3983.
- 50 A. Pei, J. Malho, J. Ruokolainen, Q. Zhou and L. A. Berglund, *Macromolecules*, 2011, **44**, 4422-4427.
- 51 Y. Tien and K. Wei, *Macromolecules*, 2001, **34**, 9045-9052.
- 52 Q. Wu, M. Henriksson, X. Liu and L. A. Berglund, *Biomacromolecules*, 2007, **8**, 3687-3692.
- 53 G. Odian, *Principles of Polymerization*, John Wiley & Sons, Inc., New Jersey, 4th edn., 2004, pp. 39-197.

- 54 S. H. Pinner, *J. Polym. Sci.*, 1956, **21**, 153-157.
- 55 M. A. Hood, C. S. Gold, F. L. Beyer, J. M. Sands and C. Y. Li, *Polymer*, 2013, **54**, 6510-6515.
- 56 A. K. Gaharwar, A. Patel, A. Dolatshahi-Pirouz, H. Zhang, K. Rangarajan, G. Iviglia, S. Shin, M. A. Hussain and A. Khademhosseini, *Biomater. Sci.*, 2015, **3**, 46-58.
- 57 Y. Li and J. A. Ragauskas, *Advances in diverse industrial applications of nanocomposites*, ed. B. Reddy, InTech, 2011, pp. 18-36.
- 58 S. Liang, W. D. Cook and Q. Chen, *Polym. Int.*, 2012, **61**, 17-22.
- 59 B. Amsden, *Soft Matter*, 2007, **3**, 1335-1348.
- 60 Y. Chandorkar, G. Madras and B. Basu, *J. Mater. Chem. B*, 2013, **1**, 965-875.
- 61 S. Liang, X. Yang, X. Fang, W. D. Cook, G. A. Thouas and Q. Chen, *Biomaterials*, 2011, **32**, 8486-8496.
- 62 M. Partini and R. Pantani, *Polym. Degrad. Stab.*, 2007, **92**, 1491-1497.
- 63 X. Gu, D. Raghavan, T. Nguyen, M. R. VanLandingham and D. Yebassa, *Polym. Degrad. Stab.*, 2001, **74**, 139-149.
- 64 M. J. Yaszemski, R. G. Payne, W. C. Hayes, R. Langer and A. G. Mikos, *Biomaterials*, 1996, **17**, 2127-2130.
- 65 Z. Ge, J. C. H. GoH, L. Wang, E. P. S. Tan and E. H. Lee, *J. Biomater. Sci., Polym. Ed.*, 2005, **16**, 1179-1192.
- 66 M. Sabir, X. Xu and L. Li, *J. Mater. Sci.*, 2009, **44**, 5713-5724.
- 67 D. E. T. Shepherd and B. B. Seedhom, *Rheumatology*, 1999, **38**, 124-132.
- 68 A. Thambyah, A. Nather and J. Goh, *Osteoarthr. Cartil.*, 2006, **14**, 580-588.
- 69 J. Lee and D. Boughner, *Circ. Res.*, 1985, **57**, 475-481.
- 70 Q. Chen, S. Liang, J. Wang and G. P. Simon, *J. Mech. Behav. Biomed. Mater.*, 2011, **4**, 1805-1818.
- 71 T. Schepull, J. Kvist, C. Andersson and P. Aspenberg, *BMC Musculoskelet. Disord.*, 2007, **8**, 116-116.

- 72 Q. Liu, J. Wu, T. Tan, L. Zhang, D. Chen and W. Tian, *Polym. Degrad. Stab.*, 2009, **94**, 1427-1435.
- 73 Q. Chen, L. Jin, W. D. Cook, D. Mohn, E. L. Lagerqvist, D. A. Elliott, J. M. Haynes, N. Boyd, W. J. Stark, C. W. Pouton, E. G. Stanley and A. G. Elefanty, *Soft Matter*, 2010, **6**, 4715-4726.
- 74 X. Yang, E. Bakaic, T. Hoare and E. D. Cranston, *Biomacromolecules*, 2013, **14**, 4447-4455.
- 75 T. Kovacs, V. Naish, B. O'Connor, C. Blaise, F. Gagné, L. Hall, V. Trudeau and P. Martel, *Nanotoxicology*, 2010, **4**, 255-270.
- 76 S. Dong, A. A. Hirani, K. R. Colacino, Y. W. Lee and M. Roman, *Nano Life*, 2012, **02**, 1241006.
- 77 M. J. D. Clift, E. J. Foster, D. Vanhecke, D. Studer, P. Wick, P. Gehr, B. Rothen-Rutishauser and C. Weder, *Biomacromolecules*, 2011, **12**, 3666-3673.
- 78 M M Pereira and N R B Raposo and R Brayner and E M Teixeira and V Oliveira and C C R Quintão and L S A Camargo and L H C Mattoso and H.M.Brand, *Nanotechnology*, 2013, **24**, 075103.
- 79 M. Jorfi and E. J. Foster, *J Appl Polym Sci*, 2015, **132**, n/a-n/a.
- 80 K. A. Mahmoud, J. A. Mena, K. B. Male, S. Hrapovic, A. Kamen and J. H. T. Luong, *ACS Appl. Mater. Interfaces*, 2010, **2**, 2924-2932.
- 81 B. Jia, Y. Li, B. Yang, D. Xiao, S. Zhang, A. V. Rajulu, T. Kondo, L. Zhang and J. Zhou, *Cellulose*, 2013, **20**, 1911-1923.
- 82 J. M. Dugan, J. E. Gough and S. J. Eichhorn, *Biomacromolecules*, 2010, **11**, 2498-2504.

**Table 1**

Main physical and mechanical properties of neat PMS and PMS/CNC composites (1, 5 and 10wt% of CNC), obtained under different curing conditions, (low and high crosslinked materials).

Curing conditions, physical and mechanical properties of PMS and nanocomposites with low degree of crosslinking (L); 120°C, 60cm Hg, 3 days								
Sample	Mannitol:Sebacic acid Ratio	Young's modulus (MPa) <sup>a</sup>	Ultimate tensile strength (MPa) <sup>a</sup>	Elongation at break (%) <sup>a</sup>	T <sub>g</sub> by DSC (°C) <sup>b</sup>	Degradation onset temperature (°C) <sup>c</sup>	Toughness (MJ/m <sup>3</sup> ) <sup>a</sup>	Hydration by mass (%)
Neat PMS	Ratio 1:1	1.8±0.3	1.2±0.7	80.0±29.0	18	227	63.6±50.0	19.6±1.5
PMS/1% CNC		2.1±0.5	2.3±0.02	147.0±31.1	18	237	187.4±46.3	20.2±0.2
PMS/5% CNC		3.0±0.3	4.6±0.6	166.0±20.5	18	230	393.5±5.2	19.3±1.1
PMS/10% CNC		6.0±0.7	5.6±0.4	119.5±18.3	17	217	389.0±86.4	21.5±0.3
Neat PMS	Ratio 1:2	7.2±0.1	4.5±0.7	35.8±3.5	16	238	81.8±5.4	14.4±1.0
PMS/1% CNC		11.1±0.6	4.6±1.2	25.6±2.5	16	239	72.5±22.6	12.0±0.3
PMS/5% CNC		14.8±1.2	6.2±1.3	25.4±2.4	10	234	94.6±23.5	11.4±0.3
PMS/10% CNC		32.3±2.6	8.5±2.0	23.4±0.04	8	233	89.3±39.1	10.4±0.8
Curing conditions, physical and mechanical properties of PMS and nanocomposites with high degree of crosslinking (H); L + 170°C, 60cm Hg, 1day								
Sample	Mannitol:Sebacic acid Ratio	Young's modulus (MPa) <sup>a</sup>	Ultimate tensile strength (MPa) <sup>a</sup>	Elongation at break (%) <sup>a</sup>	T <sub>g</sub> by DSC (°C) <sup>b</sup>	Degradation onset temperature (°C) <sup>c</sup>	Toughness (MJ/m <sup>3</sup> ) <sup>a</sup>	Hydration by mass (%)
Neat PMS	Ratio 1:1	54.4±3.3	7.0±0.6	40.5±7.0	26	263	204.4±6.3	9.0±0.2
PMS/1% CNC		54.5±1.6	13.2±2.2	94.1±14.0	24	280	757.4±238.0	8.7±0.1
PMS/5% CNC		132.5±20.6	20.1±3.4	77.0±12.6	21	274	1047.0±310.0	8.0±0.3
PMS/10% CNC		103.0±12.2	19.4±2.4	37.4±6.0	20	268	470.0±102.2	11.2±0.5
Neat PMS	Ratio 1:2	69.8±0.6	13.3±1.6	55.1±4.9	32	271	482.0±13.3	5.1±0.8
PMS/1% CNC		146.4±5.5	14.8±3.3	35.4±9.4	30	272	325.3±9.9	4.7±0.4
*PMS/5% CNC		166.5±4.0	--	--	23	277	--	2.2±1.0
*PMS/10% CNC		167.5±5.0	--	--	21	278	--	2.1±0.5

<sup>a</sup> Young's modulus was calculated from the initial slope between 0-10% of strain for low crosslinked samples and between 0-5% strain for high crosslinked samples. All the values are an average of 2-5 specimens and are determined from stress strain curves

<sup>b</sup> DSC glass transition temperatures were calculated as the midpoint of the transition in the 2<sup>nd</sup> heating run from differential scanning calorimetry traces (see Supporting Information, Figure S3)

<sup>c</sup> Determined from thermogravimetric analysis derivative peak.

\* These samples break in the clamp due to the high stiffness.

## Figure Captions

**Scheme 1.** Schematic representation of the general synthetic scheme of poly(mannitol sebacate) pre-polymer. Mannitol (1) was polymerized with sebacic acid (2) in different stoichiometries, yielding poly(mannitol sebacate) (PMS) (3) ratio 1:1 and 1:2. Note that simplified representations of the monomers and pre-polymers are shown.

**Figure 1.** Transmission electron micrograph (TEM) of CNC isolated by hydrolysis with sulfuric acid.

**Figure 2.** FTIR spectra detail of -OH band ( $3500\text{-}3200\text{ cm}^{-1}$ ) and C=O region ( $1800\text{-}1600\text{ cm}^{-1}$ ). Thick lines in the graphs correspond to low crosslinking degree samples, and thin lines correspond to high crosslinking degree samples. **Top**, for 1:1 low crosslinked (**L**) and high crosslinked (**H**) neat PMS and PMS/CNC nanocomposites and **bottom**, for 1:2 low crosslinked (**L**) and high crosslinked (**H**) neat PMS and PMS/CNC nanocomposites. The presence of these both bands confirms the formation of polyesters with the highest esterification degree for the 1:2 high crosslinked samples.

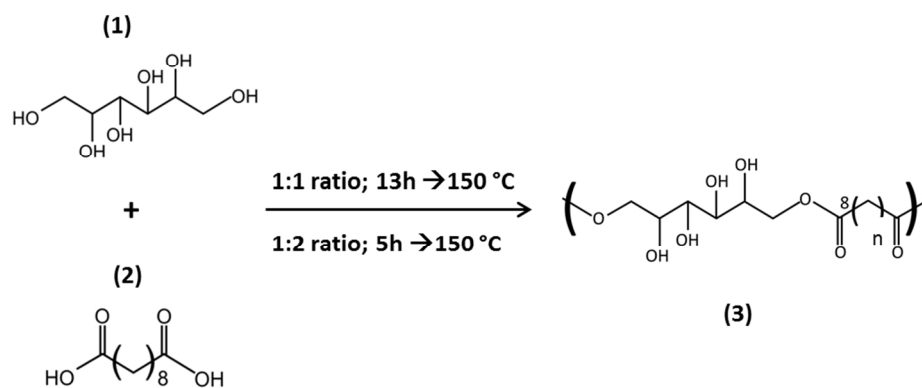
**Figure 3.** Typical tensile stress versus strain curves registered at room temperature of low Young's modulus PMS and PMS/CNC nanocomposites cured under low crosslinking conditions (**L**) from mannitol/sebacic mannitol/sebacic acid rate 1:2 (**a**). Typical tensile stress versus strain curves registered at room temperature of high Young's modulus PMS and PMS/CNC nanocomposites cured under high crosslinking conditions (**H**) from mannitol/sebacic acid rate 1:2 (**b**).

**Figure 4. Degradation** of neat PMS and PMS/CNC nanocomposites under physiological conditions (SBF at  $37\text{ }^{\circ}\text{C}$ ) monitored over 150 days. Weight loss of 1:1 neat PMS and PMS/CNC

nanocomposites with low crosslinking degree **(a)**. Weight loss of 1:1 neat PMS and PMS/CNC nanocomposites with high crosslinking degree **(b)**. Weight loss of 1:2 neat PMS and PMS/CNC nanocomposites with low crosslinking degree **(c)**. Weight loss of 1:2 neat PMS and PMS/CNC nanocomposites with high crosslinking degree **(d)**.

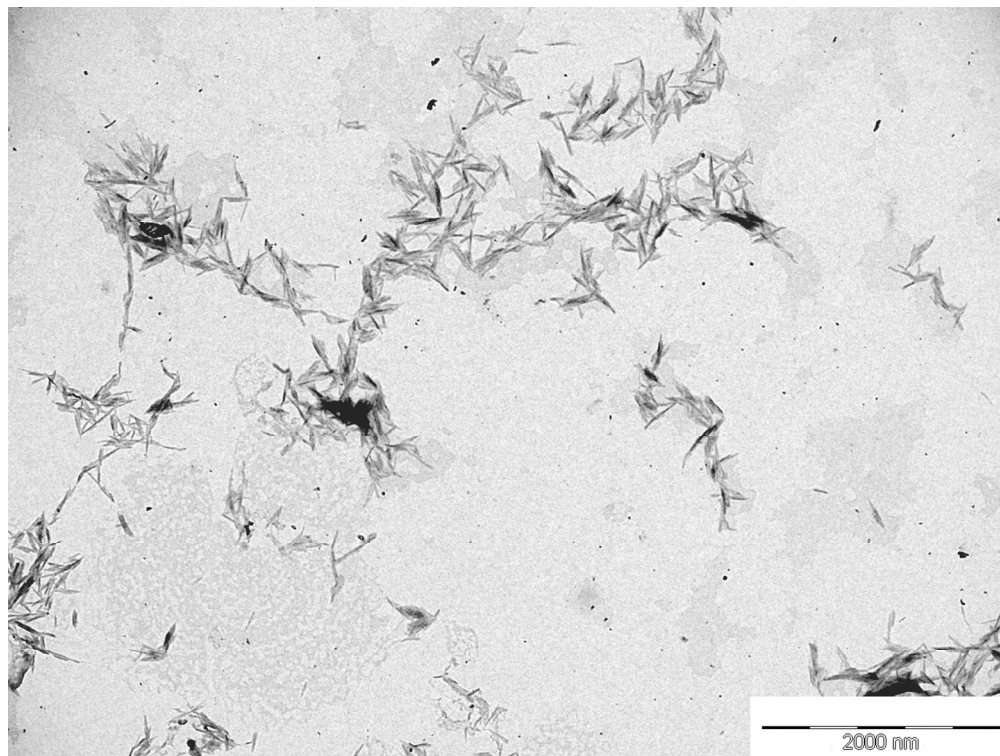
**Figure 5.** FTIR spectra detail of -OH band ( $3500\text{-}3200\text{ cm}^{-1}$ ) and C=O region ( $1800\text{-}1600\text{ cm}^{-1}$ ). Comparison between low crosslinked **(L)** and high crosslinked **(H)** 1:1 neat PMS as prepared (dry state) and after 150 days immersion in SBF **(a)**. Comparison between low crosslinked **(L)** and high crosslinked **(H)** 1:1 neat PMS as prepared (dry state) and after 150 days immersion in SBF **(b)**. New peaks centered around  $1570\text{ cm}^{-1}$  not present in the spectra of dry samples indicates the formation of salts of carboxylic acids in the SBF immersed samples during the catalysed reaction of ester groups.

**Figure 6.** Young's modulus changes between dry state (as prepared) and after immersion in SBF for different periods of time. Young's modulus of 1:1 neat PMS and PMS/CNC nanocomposites with low crosslinking degree as prepared and after 1 and 30 days of immersion in SBF **(a)**. Young's modulus of 1:1 neat PMS and PMS/CNC nanocomposites with high crosslinking degree as prepared and after 1 and 30 days of immersion in SBF **(b)**. Young's modulus of 1:2 neat PMS and PMS/CNC nanocomposites with low crosslinking degree as prepared and after 1, 30 and 150 days of immersion in SBF **(c)**. Young's modulus of 1:2 neat PMS and PMS/CNC nanocomposites with high crosslinking degree as prepared and after 1, 30 and 150 days of immersion in SBF **(d)**.

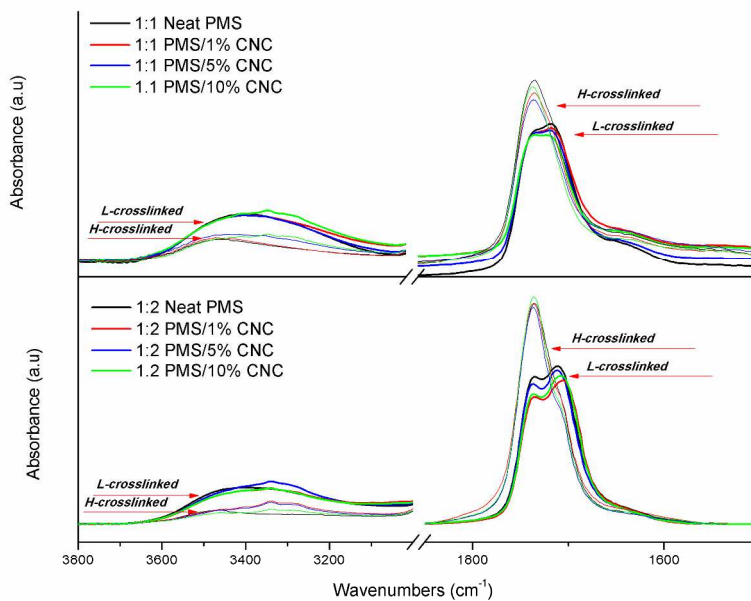


Schematic representation of the general synthetic scheme of poly(mannitol sebacate) pre-polymer. Mannitol (1) was polymerized with sebacic acid (2) in different stoichiometries, yielding poly(mannitol sebacate) (PMS) (3) ratio 1:1 and 1:2. Note that simplified representations of the monomers and pre-polymers are shown.

190x86mm (150 x 150 DPI)

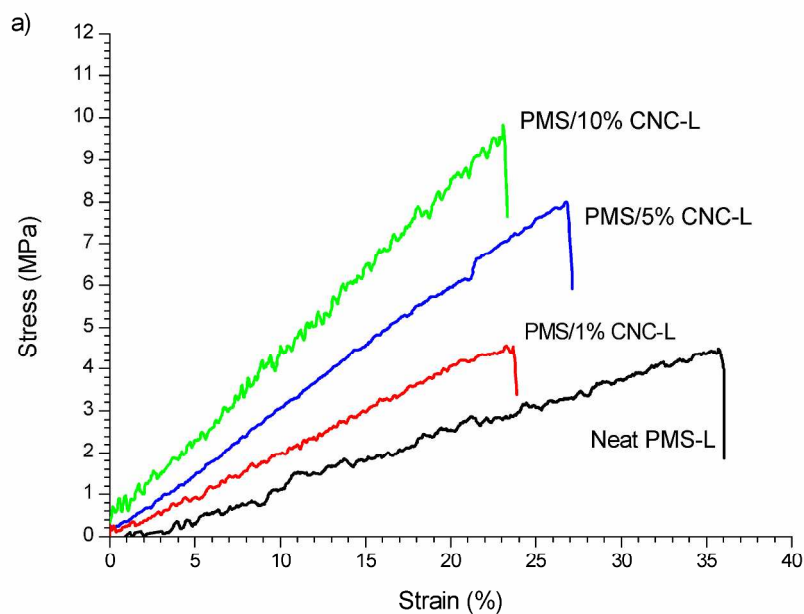


Transmission electron micrograph (TEM) of CNC isolated by hydrolysis with sulfuric acid.  
233x174mm (150 x 150 DPI)

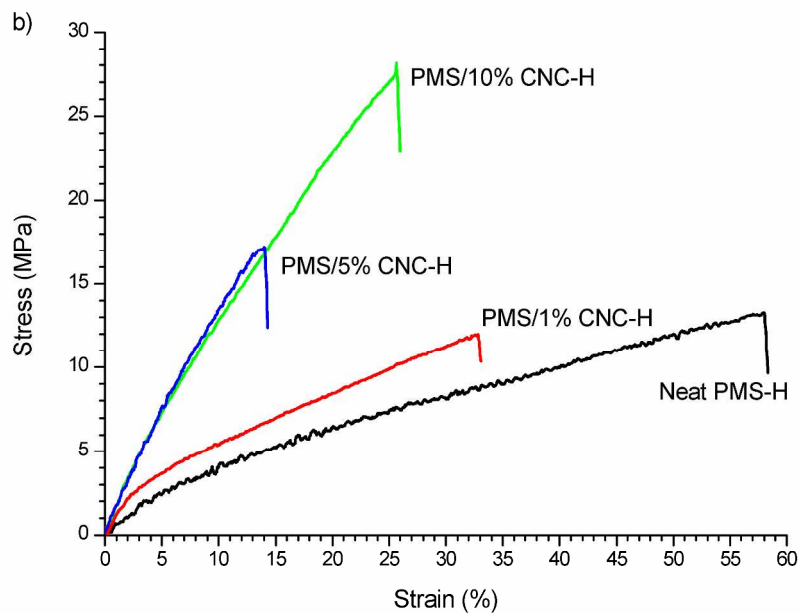


FTIR spectra detail of -OH band (3500-3200  $\text{cm}^{-1}$ ) and C=O region (1800-1600  $\text{cm}^{-1}$ ). Thick lines in the graphs correspond to low crosslinking degree samples, and thin lines correspond to high crosslinking degree samples. Top, for 1:1 low crosslinked (L) and high crosslinked (H) neat PMS and PMS/CNC nanocomposites and bottom, for 1:2 low crosslinked (L) and high crosslinked (H) neat PMS and PMS/CNC nanocomposites. The presence of these both bands confirms the formation of polyesters with the highest esterification degree for the 1:2 high crosslinked samples.

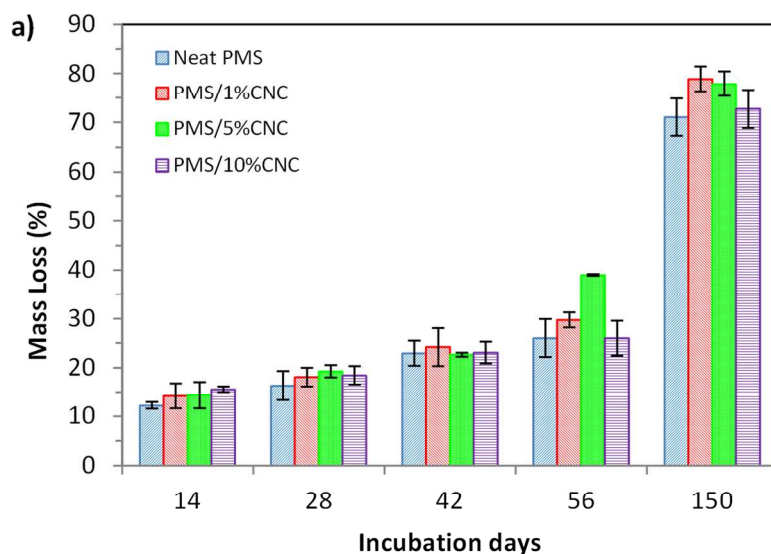
286x200mm (300 x 300 DPI)



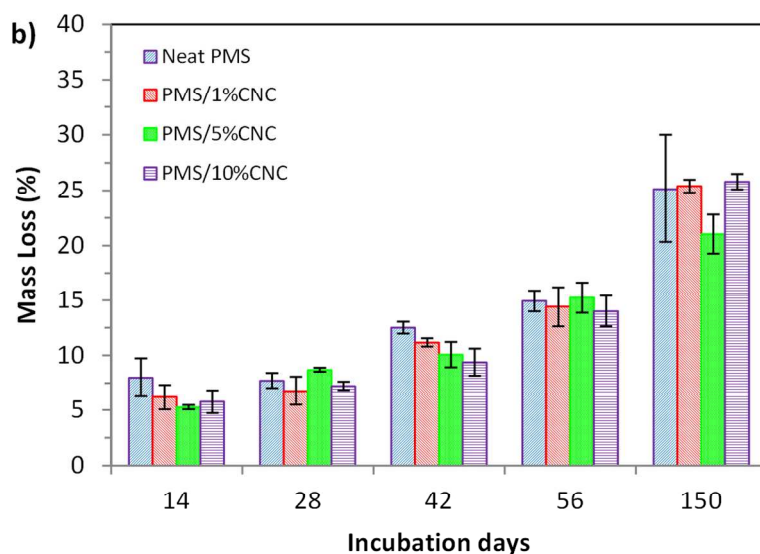
Typical tensile stress versus strain curves registered at room temperature of low Young's modulus PMS and PMS/CNC nanocomposites cured under low crosslinking conditions (L) from mannitol/sebacic mannitol/sebacic acid rate 1:2 (a). Typical tensile stress versus strain curves registered at room temperature of high Young's modulus PMS and PMS/CNC nanocomposites cured under high crosslinking conditions (H) from mannitol/sebacic acid rate 1:2 (b).  
286x201mm (300 x 300 DPI)



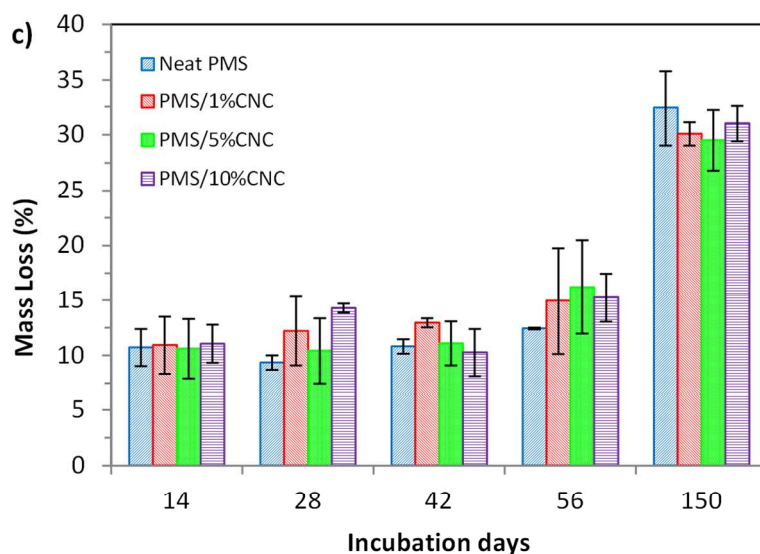
Typical tensile stress versus strain curves registered at room temperature of low Young's modulus PMS and PMS/CNC nanocomposites cured under low crosslinking conditions (L) from mannitol/sebacic mannitol/sebacic acid rate 1:2 (a). Typical tensile stress versus strain curves registered at room temperature of high Young's modulus PMS and PMS/CNC nanocomposites cured under high crosslinking conditions (H) from mannitol/sebacic acid rate 1:2 (b).  
286x201mm (300 x 300 DPI)



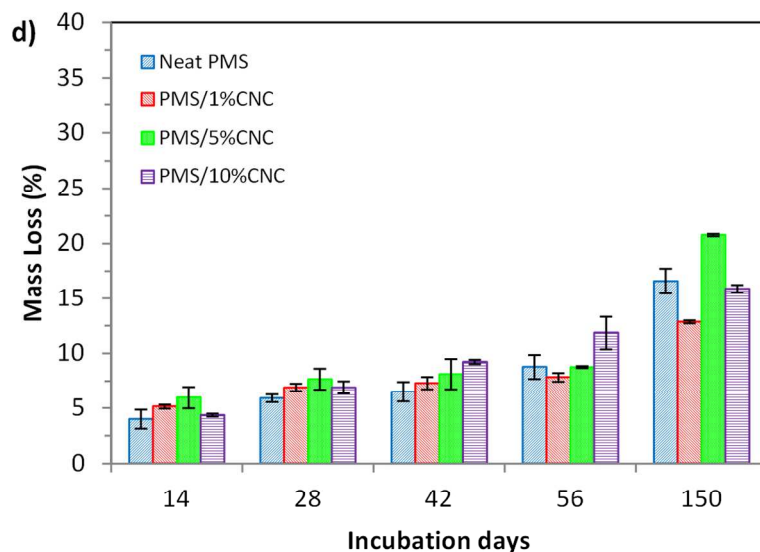
Degradation of neat PMS and PMS/CNC nanocomposites under physiological conditions (SBF at 37 °C) monitored over 150 days. Weight loss of 1:1 neat PMS and PMS/CNC nanocomposites with low crosslinking degree (a). Weight loss of 1:1 neat PMS and PMS/CNC nanocomposites with high crosslinking degree (b). Weight loss of 1:2 neat PMS and PMS/CNC nanocomposites with low crosslinking degree (c). Weight loss of 1:2 neat PMS and PMS/CNC nanocomposites with high crosslinking degree (d).  
127x76mm (300 x 300 DPI)



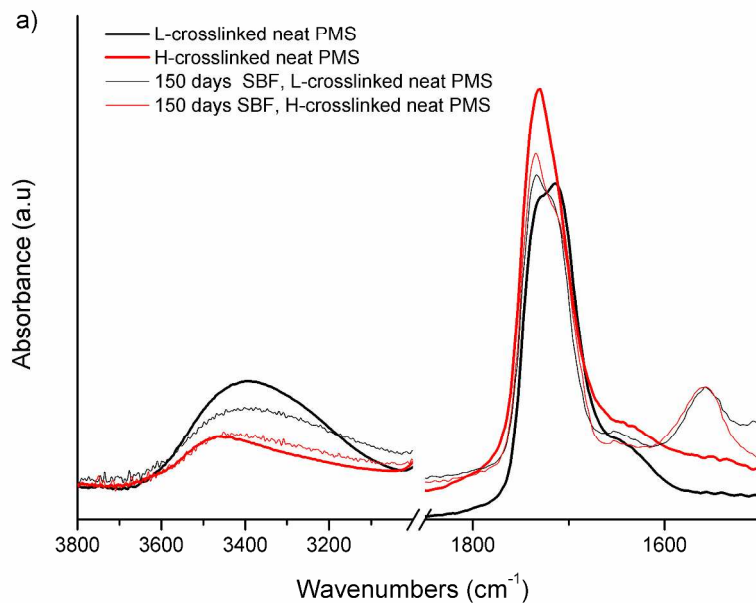
Degradation of neat PMS and PMS/CNC nanocomposites under physiological conditions (SBF at 37 °C) monitored over 150 days. Weight loss of 1:1 neat PMS and PMS/CNC nanocomposites with low crosslinking degree (a). Weight loss of 1:1 neat PMS and PMS/CNC nanocomposites with high crosslinking degree (b). Weight loss of 1:2 neat PMS and PMS/CNC nanocomposites with low crosslinking degree (c). Weight loss of 1:2 neat PMS and PMS/CNC nanocomposites with high crosslinking degree (d).  
127x76mm (300 x 300 DPI)



Degradation of neat PMS and PMS/CNC nanocomposites under physiological conditions (SBF at 37 °C) monitored over 150 days. Weight loss of 1:1 neat PMS and PMS/CNC nanocomposites with low crosslinking degree (a). Weight loss of 1:1 neat PMS and PMS/CNC nanocomposites with high crosslinking degree (b). Weight loss of 1:2 neat PMS and PMS/CNC nanocomposites with low crosslinking degree (c). Weight loss of 1:2 neat PMS and PMS/CNC nanocomposites with high crosslinking degree (d).  
127x76mm (300 x 300 DPI)

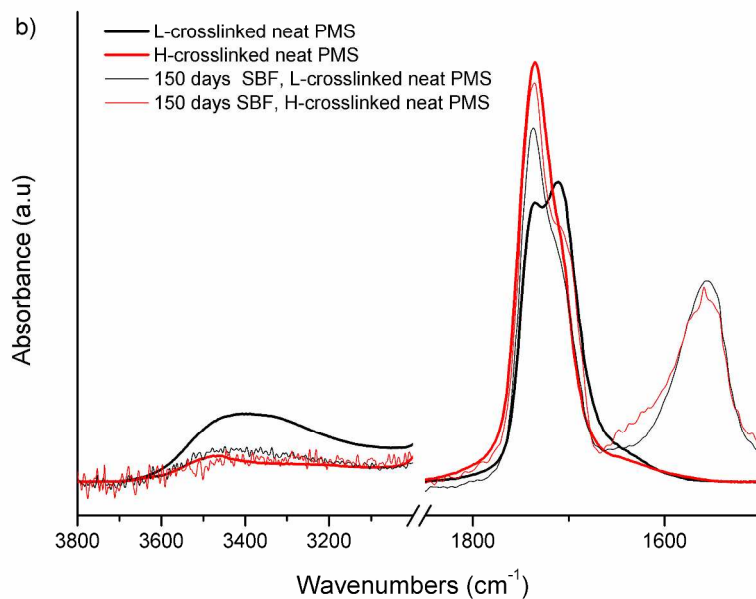


Degradation of neat PMS and PMS/CNC nanocomposites under physiological conditions (SBF at 37 °C) monitored over 150 days. Weight loss of 1:1 neat PMS and PMS/CNC nanocomposites with low crosslinking degree (a). Weight loss of 1:1 neat PMS and PMS/CNC nanocomposites with high crosslinking degree (b). Weight loss of 1:2 neat PMS and PMS/CNC nanocomposites with low crosslinking degree (c). Weight loss of 1:2 neat PMS and PMS/CNC nanocomposites with high crosslinking degree (d).  
127x76mm (300 x 300 DPI)



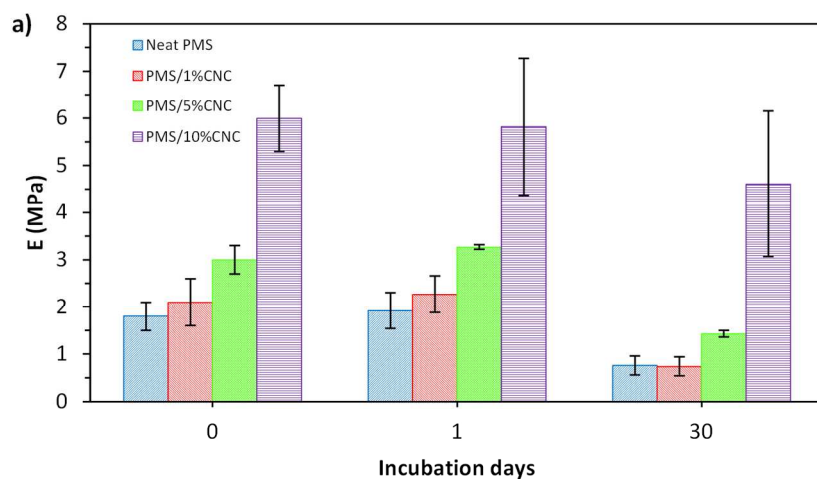
FTIR spectra detail of -OH band (3500-3200 cm<sup>-1</sup>) and C=O region (1800-1600 cm<sup>-1</sup>). Comparison between low crosslinked (L) and high crosslinked (H) 1:1 neat PMS as prepared (dry state) and after 150 days immersion in SBF (a). Comparison between low crosslinked (L) and high crosslinked (H) 1:1 neat PMS as prepared (dry state) and after 150 days immersion in SBF (b). New peaks centered around 1570 cm<sup>-1</sup> not present in the spectra of dry samples indicates the formation of salts of carboxylic acids in the SBF immersed samples during the catalysed reaction of ester groups.

287x201mm (300 x 300 DPI)



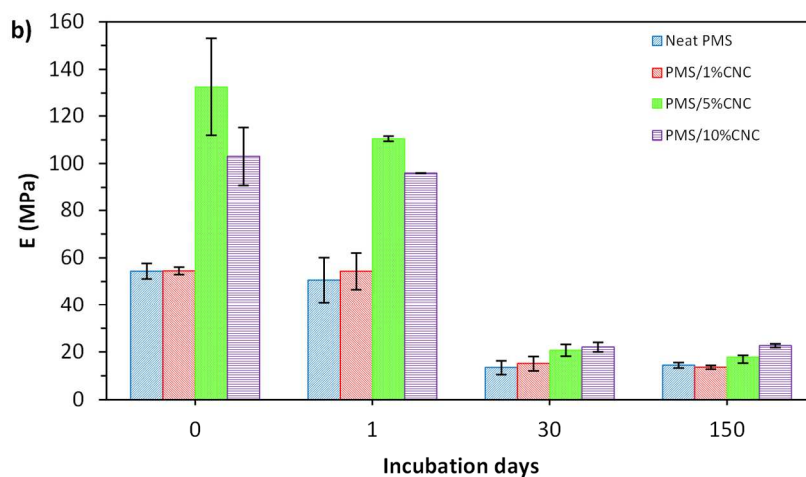
FTIR spectra detail of -OH band (3500-3200 cm<sup>-1</sup>) and C=O region (1800-1600 cm<sup>-1</sup>). Comparison between low crosslinked (L) and high crosslinked (H) 1:1 neat PMS as prepared (dry state) and after 150 days immersion in SBF (a). Comparison between low crosslinked (L) and high crosslinked (H) 1:1 neat PMS as prepared (dry state) and after 150 days immersion in SBF (b). New peaks centered around 1570 cm<sup>-1</sup> not present in the spectra of dry samples indicates the formation of salts of carboxylic acids in the SBF immersed samples during the catalysed reaction of ester groups.

287x201mm (300 x 300 DPI)



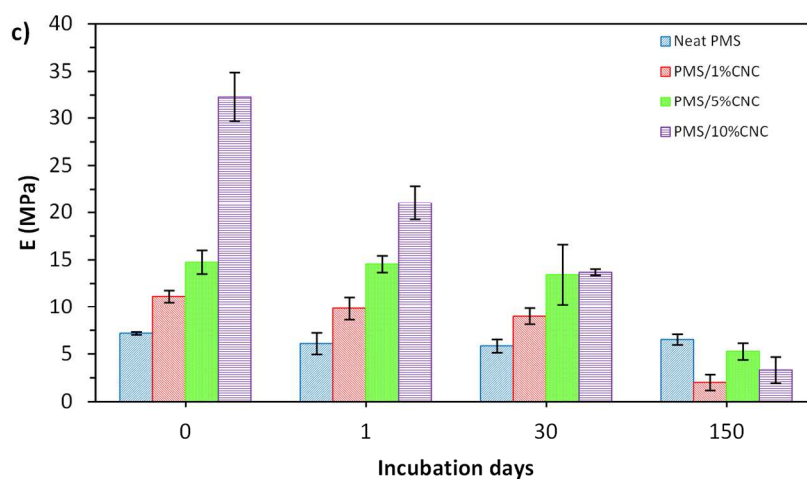
Young's modulus changes between dry state (as prepared) and after immersion in SBF for different periods of time. Young's modulus of 1:1 neat PMS and PMS/CNC nanocomposites with low crosslinking degree as prepared and after 1 and 30 days of immersion in SBF (a). Young's modulus of 1:1 neat PMS and PMS/CNC nanocomposites with high crosslinking degree as prepared and after 1 and 30 days of immersion in SBF (b). Young's modulus of 1:2 neat PMS and PMS/CNC nanocomposites with low crosslinking degree as prepared and after 1, 30 and 150 days of immersion in SBF (c). Young's modulus of 1:2 neat PMS and PMS/CNC nanocomposites with high crosslinking degree as prepared and after 1, 30 and 150 days of immersion in SBF (d).

148x76mm (300 x 300 DPI)



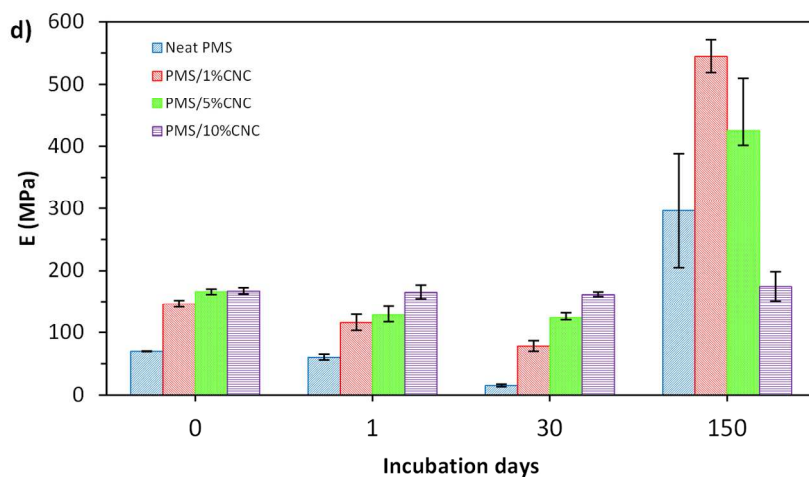
Young's modulus changes between dry state (as prepared) and after immersion in SBF for different periods of time. Young's modulus of 1:1 neat PMS and PMS/CNC nanocomposites with low crosslinking degree as prepared and after 1 and 30 days of immersion in SBF(a). Young's modulus of 1:1 neat PMS and PMS/CNC nanocomposites with high crosslinking degree as prepared and after 1 and 30 days of immersion in SBF (b). Young's modulus of 1:2 neat PMS and PMS/CNC nanocomposites with low crosslinking degree as prepared and after 1, 30 and 150 days of immersion in SBF (c). Young's modulus of 1:2 neat PMS and PMS/CNC nanocomposites with high crosslinking degree as prepared and after 1, 30 and 150 days of immersion in SBF (d).

148x76mm (300 x 300 DPI)



Young's modulus changes between dry state (as prepared) and after immersion in SBF for different periods of time. Young's modulus of 1:1 neat PMS and PMS/CNC nanocomposites with low crosslinking degree as prepared and after 1 and 30 days of immersion in SBF (a). Young's modulus of 1:1 neat PMS and PMS/CNC nanocomposites with high crosslinking degree as prepared and after 1 and 30 days of immersion in SBF (b). Young's modulus of 1:2 neat PMS and PMS/CNC nanocomposites with low crosslinking degree as prepared and after 1, 30 and 150 days of immersion in SBF (c). Young's modulus of 1:2 neat PMS and PMS/CNC nanocomposites with high crosslinking degree as prepared and after 1, 30 and 150 days of immersion in SBF (d).

148x76mm (300 x 300 DPI)



Young's modulus changes between dry state (as prepared) and after immersion in SBF for different periods of time. Young's modulus of 1:1 neat PMS and PMS/CNC nanocomposites with low crosslinking degree as prepared and after 1 and 30 days of immersion in SBF (a). Young's modulus of 1:1 neat PMS and PMS/CNC nanocomposites with high crosslinking degree as prepared and after 1 and 30 days of immersion in SBF (b). Young's modulus of 1:2 neat PMS and PMS/CNC nanocomposites with low crosslinking degree as prepared and after 1, 30 and 150 days of immersion in SBF (c). Young's modulus of 1:2 neat PMS and PMS/CNC nanocomposites with high crosslinking degree as prepared and after 1, 30 and 150 days of immersion in SBF (d).

148x76mm (300 x 300 DPI)